LIMNOLOGY and OCEANOGRAPHY: METHODS

ASLO

Limnol. Oceanogr.: Methods 18, 2020, 585–598

doi: 10.1002/lom3.10386

Introducing the TiDyWAVE field flume: A method to quantify natural ecosystem resilience against future storm waves

J. C. de Smit,[1,2]* **M. G. Kleinhans**,[2] **T. Gerkema**,[1] **K. R. Timmermans**,[1] **T. J. Bouma**[1,2]

[1]NIOZ Royal Netherlands Institute for Sea Research, Department of Estuarine and Delta Systems, Utrecht University, Yerseke, The Netherlands

[2]Faculty of Geosciences, Utrecht University, Utrecht, The Netherlands

Abstract

Coastal ecosystems are increasingly threatened by global change. Insight in their resilience against increased storminess is needed for their application in nature-based coastal defense schemes. This is often gained from flume experiments. Laboratory flumes provide excellent hydrodynamic control, but are restrictive in that it is extremely difficult to experiment on ecosystems with a naturally developed stability. Field flumes resolve the latter, but are limited to unidirectional currents. This study introduces an easily deployable field flume that mimics the near-bed water motion of waves: the Tidal Dynamics WAVE flume (the TiDyWAVE). The hydrodynamics of the TiDyWAVE are assessed and compared to natural waves. We also compare it with a more traditional unidirectional flow channel by measuring the erodibility (u_{cr}) of (1) bare sediments of which u_{cr} can be calculated and (2) a seagrass meadow. The TiDyWAVE can generate peak oscillatory currents up to 0.32 m s^{-1} with a maximum wave period of 3.5 s, corresponding to 0.42 m high waves for a water depth of 3 m. u_{cr} measurements showed that bed shear stress in the TiDyWAVE mimics field waves well. In accordance with theory, the observed u_{cr} on bare sediment is consistently lower for oscillatory flow compared to unidirectional currents. On *Thalassia testudinum*, u_{cr} under unidirectional currents increases 3.5 times faster with increasing blade area than under oscillatory flow. The difference in hydrodynamic sheltering of the seabed by flexible vegetation under currents vs. waves emphasizes the need for imposing representative hydrodynamics to study hydrodynamic thresholds of coastal ecosystems.

Global change is increasingly threatening coastal populations living around the world. Yet coastal areas often house densely populated and rapidly growing urban areas, especially in the least developed countries (McGranahan et al. 2007). Engineered coastal protection is often expensive, and not climate change resilient. Hence, there is a growing desire and need to use coastal ecosystems for both nature-based flood defense schemes (e.g., see Temmerman et al. 2013) and shoreline stabilization (James et al. 2019). This makes it of pivotal importance to quantify the resilience of coastal ecosystems against disturbances like storm attacks (Bouma et al. 2014). Many coastal ecosystems are known to exhibit sudden shifts between stable states, triggered by regular exceedance of a critical environmental threshold, with hydrodynamic forces potentially playing a key role in the exceedance event (van der Heide et al. 2007; Bouma et al. 2016). Wave conditions are projected to change for 50% of the global coastlines due to climate change (Morim et al. 2019), which given the sensitivity of coastal ecosystems to hydrodynamic threshold exceedance could potentially lead to state shifts. Nevertheless, only very few studies test ecosystem performance under hydrodynamic threshold conditions, often relying on laborious and potentially expensive ecosystems transplantation methods (see e.g., Rupprecht et al. 2017; Marin-Diaz et al. 2019). To be able to quantify to which extent various coastal ecosystems can persist under potential future wave conditions, there is a need for an easily applicable method to quantify the hydrodynamic thresholds of ecosystem collapse.

Flume experiments are a commonly used method to gain insight in hydrodynamic thresholds of aquatic ecosystems. While laboratory flumes provide excellent control over the hydrodynamics, the studied ecosystem typically needs to be simplified in some aspects. For example, mimics have often been used to represent vegetation in studying vegetation-hydrodynamics interactions (see e.g., Ghisalberti and Nepf 2002). Changes in sediment properties such as

*Correspondence: jaco.de.smit@nioz.nl

consolidation due to desiccation and vibration during transport (Tolhurst et al. 2000) and mixing when placing sediment in the flume (Widdows et al. 1998) have been shown to potentially influence sediment erodibility. Thus, unless expensive and laborious large-scale ecosystem transplantation methods are used (Möller et al. 2014; Rupprecht et al. 2017), such ecosystem simplifications and alterations strongly restrict our ability to gain quantitative insight in the hydrodynamic thresholds of coastal ecosystems when using laboratory flumes.

In contrast to laboratory flumes, field studies provide access to naturally developed intact ecosystems. However, field studies lack the hydrodynamic control that laboratory flumes provide. This gives rise to some major logistic challenges when studying hydrodynamic thresholds. One must wait for a storm to occur that is strong enough to pass the hydrodynamic threshold, which might be very rare, and hence may likely not occur during the measurement period given that the ecosystem has not collapsed before. Yet when the perfect storm finally is predicted to occur, it will be challenging to timely install all equipment robustly enough to conduct process measurements under these potentially hazardous conditions.

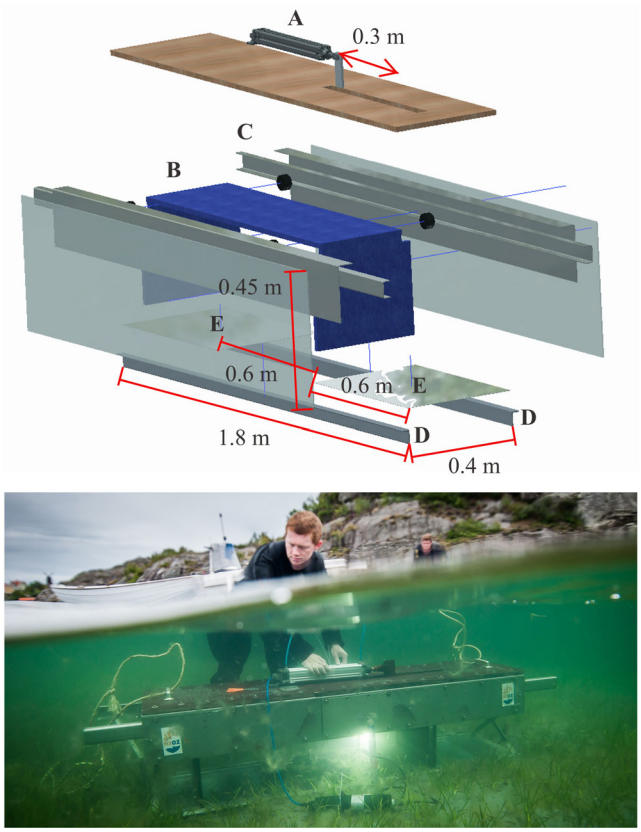

Fig 1. Top: Exploded view of the TiDyWAVE. The pneumatic piston (**A**) drives two connected paddles (**B**) that oscillate 0.3 m along a rail (**C**), generating an oscillatory flow over the 0.6 m test section. The flume walls are pressed 0.05 m into the bottom (**D**), and two 0.6 m bottom plates which extend 0.15 m beyond the paddle limits prevent scouring. Bottom: In situ deployment of the TiDyWAVE on a seagrass bed (photo credit: Eduardo Infantes).

Field flumes may offer a way forward in gaining quantitative insight in hydrodynamic collapse thresholds of naturally developed and fully undisturbed coastal ecosystems, in that they can generate controlled hydrodynamics in situ. While field flumes typically do not provide the same degree of hydrodynamic accuracy as laboratory flumes, they do provide sufficient physical control to study ecosystem resilience to specific (future) hydrodynamic conditions. To our knowledge, field flumes are currently limited to unidirectional flow channels only (see e.g., Scoffin 1968; Amos et al. 1992; Widdows et al. 2007). In coastal environments however, waves are generally the more dominant influence on morphodynamics compared to currents (Callaghan et al. 2010; Nyberg and Howell 2016), and affect sediment motion in ecological structures differently than currents. For example, flexible vegetation bends under currents, creating a skimming flow over the blades while slowing down the current inside the canopy (Järvelä 2005; Peralta et al. 2008) and reducing the exchange between the canopy and the water column (Koch and Gust 1999). Under waves however, flexible vegetation makes a periodic swooping motion (Bouma et al. 2010; Luhar et al. 2017), decreasing their protective effect on the sediment, thereby increasing the exchange between the canopy and water column (Koch and Gust 1999) and making it more likely for the system to start eroding.

Given the importance of waves in coastal ecosystems, there is a need for field flumes capable of generating the characteristic near-bed hydrodynamics of waves to gain quantitative insight in the hydrodynamic thresholds of coastal ecosystem stability. In this paper, we introduce a novel field flume, called the Tidal Dynamics WAVE flume (hereafter referred as the TiDyWAVE), that generates oscillatory flow designed to impose the near-bed hydrodynamics of waves in shallow water. To assess the performance of the TiDyWAVE, we first analyze the hydrodynamic properties of the flume and compare this with natural wave dynamics. Secondly, we also test the TiDyWAVE by comparing in-situ critical erosion thresholds on a range of bare and vegetated sediments to those obtained by a more traditional unidirectional flow channel, the TiDyFLOW (James et al. 2019).

Materials and methods

TiDyWAVE field-flume: Design, aims, and considerations

The TiDyWAVE (Fig. 1) generates an oscillatory flow by periodic motion of a paddle in a semi-enclosed flow tunnel that is only open at the bed. This oscillatory flow design is based on the proven design of larger laboratory-based oscillatory flow channels, also known as oscillatory trays or U-tubes,

Table 1. Overview of the locations of wave buoys in the Western Scheldt and Wadden Sea, the Netherlands, and period for which 10-min significant wave height data was taken for comparison with the TiDyWAVE. Source: MyOcean, http://www.emodnet-physics.eu/Map/.

Buoy name	Location (lat, long)	Measurement range
Amelander 61	53.320, 5.576	Nov 2011–Mar 2018
Wierumerwad 2	53.410, 6.064	Jun 2015–Mar 2018
Hansweert	51.448, 3.999	Sep 2014–Mar 2018
Terneuzen	51.359, 3.745	June 2015–Mar 2018

which have previously been used to study the near-bed hydrodynamics of full-scale ocean waves (see e.g., Bagnold 1946; O'Donoghue and Clubb 2001; Ribberink et al. 2008). Oscillatory channels generate a fully oscillatory flow, while in the nearshore zone outside the boundary layer the horizontal and vertical velocity are of similar magnitude. In the near-bed zone however the flow is almost fully oscillatory, even in the transitional wave regime (Jonsson and Carlsen 1976). This makes oscillatory channels suitable devices to study processes, which are governed by the hydrodynamic conditions in the bottom boundary layer, such as the entrainment of sediment particles. For the TiDyWAVE to be a successful tool to study hydrodynamic thresholds in situ, it needs to (1) be capable of generating a range of wave conditions typical for normal and extreme conditions in the area of interest and (2) remain small and light enough to be portable and easily deployable from small vessels. The configuration of the TiDyWAVE as presented in this paper is aimed to be primarily used in shallow subtidal coastal areas, specifically estuaries and bays where wave generation is either fetch or depth limited, with water depths ranging from 0.5 to 3 m. The minimum depth depends on the outside wave conditions, as the flume roof must remain submerged during deployment. The current dimensions of the TiDyWAVE were chosen as a trade-off between portability, so that the flume can be carried by two persons, and the minimum wave strength that needs to be generated.

Physical design conditions: Assessing near-bed oscillatory flow in the field and in TiDyWAVE

To assess the ideal wave generation capabilities of the TiDyWAVE, significant wave height and period measurements were analyzed for four sites: two in the Wadden Sea and two in the Western Scheldt, downloaded from EMODnet (Table 1). The range in observational length varied between nearly three and nearly 8 yr, with the interval between measurement bursts being 10 min. These sites were selected to include contrasting wave conditions, so that a more general comparison between the maximum waves generated by the TiDyWAVE and the range of natural wave conditions can be made. The wave buoys in the Wadden Sea are located on shoals, and the wave buoys in the Western Scheldt are located near the edge of tidal flats. As the near-bed velocity corresponding to the wave height and period depends on the water depth, which will vary between sites, tidal cycle, and storm surge height, a direct comparison cannot be made. However, the combination of these contrasting locations provides a general overview of possible wave conditions in estuarine and shallow coastal environments. Waves in the Western Scheldt are generally fetch-limited with fetches in the order of 5–20 km. In the Wadden Sea, the waves are generally depth-limited, as during high tide the water depth on the tidal flats is in the order of 0.5–2 m.

We used linear wave theory to calculate both typical and extreme wavelengths and near-bed oscillatory velocities that can occur in the field. While linear wave theory is strictly only valid for small-amplitude sinusoidal waves, it is generally applied even in the surf zone with shoaling waves, for which the error is in the order of 20% (Guza and Thornton 1980). Given that shoaling dynamics are sensitive to the bottom profile, which makes it sensitive to an arbitrary location, and that the purpose of this calculation does not require optimal accuracy, we consider linear wave theory to be a sufficiently accurate first approximation for comparing the maximum orbital velocity of the TiDyWAVE with natural conditions.

The peak near-bed orbital velocity $u_{\max}$ can be calculated for the range of wave heights H (i.e., twice the amplitude) and wave periods T as:

$$u_{\max} = \frac{\omega H}{2\sinh[kd]} \tag{1}$$

where $\omega = \frac{2\pi}{T}$ is the radial frequency (rad s^{-1}) and $k = \frac{2\pi}{L}$ is the wave number (m^{-1}) where L is wavelength (m), and d is water depth to be mimicked in the TiDyWAVE (m). The wavelength is calculated from the dispersion relation:

$$L = \frac{g\mathrm{T}^2}{2\pi}\tanh\left[\frac{2\pi d}{L}\right] \tag{2}$$

where g is gravitational acceleration (9.81 m s^{-2}). This equation is solved iteratively. Since the TiDyWAVE does not induce breaking waves, the upper wave height limit is defined as the wave breaking limit. The wave breaking limit for wave steepness can be calculated with the Miche-criterion (Miche 1944):

$$\left(\frac{H}{L}\right)_{br} = 0.142\tanh[kd] \tag{3}$$

which applies for both deep water ($d/L > ½$), where it approaches $\left(\frac{H}{L}\right)_{\mathrm{br}} = 0.142$ and shallow water ($d/L < ½$), where it approaches $\left(\frac{H}{d}\right)_{\mathrm{br}} = 0.78$.

To calculate the wave height corresponding to the wave motion induced in the TiDyWAVE, Eq. 1 can be rewritten as:

$$H = \frac{2u_{\max}\sin h[kd]}{\omega} \quad (4)$$

where in this case u_{max} is the peak oscillatory velocity (i.e., the maximum velocity during a wave cycle) that the flume can generate, which was measured at 0.15 m above the bed.

Construction details of the TiDyWAVE field-flume

The TiDyWAVE consists of two main parts: the outer shell (l × h × w = 1.8 × 0.5 × 0.4 m) to which the piston and sensors are attached (Fig. 1A), and the two paddles which are internally coupled by a roof (l × h × w = 1.2 × 0.35 × 0.4 m; Fig. 1B) and moved along a rail attached to the outer shell (Fig. 1C). The paddles and roof have rubber edges to make a seal with the outer shell, preventing leakage and ensuring that the water motion is as uniform over the cross-section and as equal to the paddle motion as possible. The flume walls are pressed 0.05 m into the sediment to prevent scouring (Fig. 1D). To prevent sediment scouring below the wave paddles, an aluminum bottom plate is mounted below both paddles, extending 0.15 m beyond the paddle stroke on each side (Fig. 1E). In this configuration, see Table 2 for key parameters, the total weight of the flume is approximately 60 kg. This allows for transportation with a small vessel and deployment and repositioning on the seabed by two persons, making the present configuration of the flume suitable for conducting many repeated experiments along ecological gradients.

A pneumatic piston drives the two paddles over a maximum stroke length of 0.3 m, generating an up to 0.32 m s^{-1} oscillatory flow over the 0.6 m test section. An oversized pneumatic piston providing enough force to generate the desired oscillatory velocities on bed slopes upwards of 45°, i.e., beyond the angle of repose for most sediments, was used to remove any influence from field waves or bed slope on the paddle motion. The maximum bed slope at which the flume can operate is thus limited by (1) slope gradient, as there cannot be any gaps in the sealing with the seabed inducing scouring, and (2) flume anchoring, as the flume itself should not slide. As the TiDyWAVE is an enclosed system, it is prone to internal wave reflections. Therefore, the pneumatic piston was programmed to induce only the minimum necessary acceleration required to reach the desired peak oscillatory velocity—wave period combinations. Air can be provided either from a compressor or from a diving bottle, as the pneumatic piston can operate at pressures ranging from 6 to 16 bar. At the maximum velocity, the air consumption is approximately 150 L min^{-1}, so a single standard 2500-L diving bottle with be used up in approximately 15 to 20 min at this velocity setting. In our tests, one 2500-L diving bottle allowed for at least 5 erodibility measurements (see Sections 1.5 and 1.7), for which the flow is increased stepwise for approximately 10 min and kept at the critical velocity for erosion for at least 1 min. Two diving bottles provided enough air for a full day of fieldwork.

Table 2. Key parameters of the TiDyWAVE in the configuration as presented in this study.

External dimensions (l × w × h)	1.8 × 0.4 × 0.5 m
Internal dimensions (l × w × h)	1.2 × 0.35 × 0.4 m
Weight	60 kg
Measurement section dimensions (l × w)	0.6 × 0.35 m
Piston force	1000 N at 6 bar
Piston stroke length	0.3 m
Piston air consumption	Max. 150 L min^{-1}
Oscillatory velocity range	< 0.09 to 0.32 m s^{-1}
Wave period range	2.5 to 8 s

Characterizing the hydrodynamics of the TiDyWAVE

To assess the hydrodynamic characteristics of the TiDyWAVE, we have measured velocity profiles and turbulence spectra of a range of velocity settings with a wave period of approximately 4 s. The wave period is influenced by the piston force and the inertia of the moving water, and increases from 3.5 to 4 s with corresponding decreasing peak velocity from 0.32 to 0.09 m s^{-1}. The initial peak oscillatory velocity was set at 0.09 m s^{-1} and was increased stepwise until the travel of the cylinder became length limited at 0.32 m s^{-1}. Lower peak oscillatory velocities are possible, but the effect of internal paddle friction on the water motion becomes relatively larger. This potentially makes measurements at very low velocity settings less accurate.

The vertical flow profile was measured in the middle of the measurement section with an Acoustic Doppler Velocimeter Profiler (ADV-Profiler, Nortek®). The ADV-profiler was inserted from the side at elevations above the bed of 2, 8, and 15 cm. To ensure that measured peak oscillatory velocities and turbulence spectra are accurate, the flow velocity was measured at 50 Hz for a duration of 3 min over a 12 × 7 mm horizontally positioned cylindrical volume that is divided in three 4 × 7-mm cells around the focal area of the ADV-profiler's receptors. For the velocity time series and wave height calculations from linear wave theory, the measured flow at 0.15 m elevation, i.e., in the free stream regime, was used. The horizontal flow profile of the ADV-profiler was averaged over space and triangulated:

$$u_x = \sqrt{u_{x,\mathrm{adv}}{}^2 + u_{z,\mathrm{adv}}{}^2} \quad (5)$$

where u_x is total instantaneous flow velocity in the x-direction and $u_{x,adv}$ and $u_{z,adv}$ are profile-averaged flow velocities in the ADV's x and z axis directions (i.e., parallel and perpendicular to the main flow direction respectively, as the ADV is inserted sideways). This was done because there can be some minor flexing of the flume walls during deployment due to their lightweight design. Therefore, slight changes in the ADV

probe orientation may have occurred during and between measurements. To assess whether there are any unwanted differences in oscillatory flow over the height of the flume channel due to unrealistic boundary layer height, the vertical velocity profile was calculated using the root mean square velocity:

$$u_{\mathrm{rms}} = \sqrt{\frac{1}{n}\sum_{i=1}^{n}\left(u_{x,i}{}^{2}\right)} \tag{6}$$

where n is the total number of velocity samples of a complete time series. This was compared with the theoretical thickness of the boundary layer multiplied by 2, as this indicates the height at which bottom shear stress influences the vertical velocity profile (Van Rijn 1993, chapter 2). The boundary layer thickness was calculated as (Jonsson and Carlsen, 1976):

$$\delta_w = A_{\mathrm{max}}\left[0.072\left(\frac{A_{\mathrm{max}}}{ks}\right)^{-0.25}\right] \tag{7}$$

where A_{max} is the peak orbital excursion (m), equal to $\frac{u_{x,\mathrm{max}}T}{2\pi}$, where $u_{x,\mathrm{max}}$ is the peak oscillatory velocity in x-direction and ks is the equivalent bed roughness for waves, which was calculated using Eq. 13–17.

To validate the oscillatory velocity time series in the TiDyWAVE, ADV measurements were also conducted in the field during wave conditions where the significant orbital velocity of the natural wave was similar to the mean oscillatory velocity of the waves in the TiDyWAVE at 0.32 m s^{-1}. The ADV was placed in 2-m deep water, and measured orbital velocity at 8 Hz at the same height as the ADV-profiler in the TiDyWAVE, i.e., 0.15 m above the bed.

Erosion threshold measurements on bare sediments, using TiDyWAVE and TiDyFLOW

To assess whether the production of shear stress by the TiDyWAVE is representative of that of natural waves with similar oscillatory velocities, the critical free stream velocity (u_{cr}) for the onset of incipient motion, here defined as the movement of enough particles to cause a significant change in bed configuration such as ripple formation, was measured on three types of artificial sediment of which u_{cr} can be calculated. For comparison, similar measurements were conducted using a more traditional unidirectional flow channel, the TiDyFLOW (James et al. 2019). For the TiDyFLOW, u_{cr} was defined as the mean flow velocity during which incipient motion was observed. For the TiDyWAVE u_{cr} is a peak oscillatory velocity, here defined as the mean of all oscillatory velocity peaks during which incipient motion was observed. These have been extracted from the ADV data by locating all velocity peaks with a maximum peak prominence of 0.4 m s^{-1}, to remove any ADV noise peaks that made it through initial filtering, and a minimum time between individual peaks of a quarter wave period to remove turbulence-induced velocity peaks. u_{cr} was measured by gradually increasing flow velocity and peak oscillatory velocity in the TiDyFLOW and the TiDyWAVE respectively until incipient motion was observed visually. Visual observation is inherently subjective, but as bed-load transport is proportional to flow velocity to the power of 3, the difference in flow velocity between the stochastic movement of a small number of particles and the continuous movement of many particles remains small. Therefore, visual observations are sufficiently accurate for determining incipient motion at the detail required for ecological studies.

The artificial sediments consisted of three types. A moderately sorted sediment (median grain size D_{50} = 3.5 mm, sediment density ρ_{s} = 1200 kg m^{-3}) was used to quantify the effect of hiding-exposure processes. A unimodal well-sorted sediment of 3-mm-diameter cylindrically shaped grains (ρ_s = 1200 kg m^{-3}) was used to quantify the effect of an irregular shape. Lastly, a unimodal well-sorted sediment with 2.5-mm spherical grains (ρ_{s} = 1065 kg m^{-3}) was used to serve as a reference, as sediment transport theory is strictly only valid for spherical grains. These low-density sediments were chosen because they are particularly sensitive to vertical flow fluctuations generated by pressure gradients in the flow field, which may be stronger than those under natural waves due to the enclosed design of the TiDyWAVE. Pressure forces are inherently accounted for in empirical sediment transport predictors, which also have been calibrated to flume measurements on similar low-density particles (see Camenen et al. 2009 and references therein for sediment entrainment under oscillatory flow). Therefore, any differences between natural waves and oscillatory flow generated by the TiDyWAVE will be exacerbated on low-density sediments.

Validating measured erosion thresholds by calculating u_{cr} from shields theory

To assess the validity of measured u_{cr}, it was compared with u_{cr} calculated from Shields theory. For oscillatory flow from the TiDyWAVE it can be calculated as (Van Rijn 1993, chapter 2):

$$u_{\mathrm{cr}} = \sqrt{\frac{\tau_{cr}}{\frac{1}{2}\rho f_w}} \tag{8}$$

where u_{cr} is the peak oscillatory velocity, τ_{cr} is the critical bed shear stress (N m^{-2}), ρ is fluid density (1000 kg m^{-3} for water), and f_{w} is a dimensionless friction factor. Critical bed shear stress can be calculated for both unidirectional and oscillatory flow as:

$$\tau_{\mathrm{cr}} = \theta_{cr}(\rho_s - \rho)gD_{50} \tag{9}$$

where θ_{cr} is the critical Shields number, which can be calculated as (Soulsby 1997, chapter 6):

$$\theta_{cr} = \frac{0.3}{1+1.2D^*} + 0.055\left[1-\exp\left(-0.02D^*\right)\right] \quad (10)$$

where D^* is the dimensionless grain size, which can be calculated as:

$$D^* = D_{50}\left[\frac{Rg}{\upsilon^2}\right]^{\frac{1}{3}} \quad (11)$$

where R is the relative submerged density of the sediment ($R = \frac{\rho_s - \rho}{\rho}$) and υ is kinematic viscosity (10^{-6} m^2 s^{-1} for 20°C water). The friction factor f_w for rough turbulent flow has been calculated as (Swart 1976):

$$f_w = \exp\left[-5.977 + 5.213^*\left(\frac{A_{max}}{ks}\right)^{-0.194}\right] \quad (12)$$

The equivalent roughness height ks is calculated for both unidirectional and oscillatory flow as (Camenen et al. 2009):

$$ks = D_{50}\left[0.6 + 2.4\left(\frac{\theta}{\theta_{cr,ur}}\right)^{1.7}\right] \quad (13)$$

where $\theta_{cr,ur}$ is the upper-regime limit, i.e., the limit where ks is no longer a function of grain size only, which is calculated as:

$$\theta_{cr,ur} = 0.115\frac{{F_{rw}}^{1.2}}{{W_{s^*}}^{0.4}R^{0.3}} \quad (14)$$

where F_{rw} is the equivalent Froude number for waves:

$$F_{rw} = \frac{u_{cr}}{\sqrt{g\sqrt{\nu T}}} \quad (15)$$

and W_{s^*} is the dimensionless settling velocity (Camenen et al. 2009):

$$W_{s^*} = \left[\frac{R^2}{g\nu}\right]^{1/3} W_s \quad (16)$$

where W_s is the settling velocity (m s^{-1}) (Soulsby 1997, chapter 8):

$$W_s = \frac{\nu}{D_{50}}\left[\sqrt{10.36^2 + 1.049{D_*}^3} - 10.36\right] \quad (17)$$

For unidirectional currents from the TiDyFLOW, u_{cr} can be calculated as (Van Rijn 1993, chapter 2):

$$u_{cr} = \sqrt{\frac{\tau_{cr}C^2}{\rho g}} \quad (18)$$

where u_{cr} mean flow velocity, τ_{cr} is critical shear stress calculated using Eq. 9–11, and C is the Chézy roughness coefficient (m$^{0.5}$ s^{-1}), which is can be empirically approximated for hydraulic rough flow as (Van Rijn 1993, chapter 2):

$$C = 18\log_{10}\frac{12d}{ks} \quad (19)$$

where d is water depth (m), which in the case of the TiDyFLOW is defined as the height at which flow is generated (0.1 m), and ks is the equivalent roughness height which for unidirectional flow is calculated using Eq. 13 with $\theta_{cr,ur}$ calculated for unidirectional flow as (Camenen et al. 2006):

$$\theta_{cr,ur} = 1.18\frac{F^{1.4}}{{W_{s^*}}^{0.7}} \quad (20)$$

where F is the Froude number for unidirectional flow:

$$F = \frac{u_{cr}}{\sqrt{gd}} \quad (21)$$

In situ erosion threshold measurements within seagrass vegetation

Erosion threshold measurements were also conducted in situ on a *Thalassia testudinum* bed in Lac Bay, Bonaire (12°06′ N; 68°13′ W), to assess the difference in sediment sheltering by flexible vegetation between unidirectional currents and oscillatory flow. Both flumes were placed on various locations inside the meadow, covering a range of shoot densities between 480 and 800 shoots per square meter and two shoot lengths; undisturbed (0.181 ± 0.038 m) and grazed (0.043 ± 0.016 m). Additional control measurements were conducted on bare sediments. Like the erosion threshold measurements on bare artificial sediments, flow velocity and peak oscillatory velocity were gradually increased until incipient sediment motion was observed. u_{cr} was measured three times on each location and averaged.

Assessment

Flume hydrodynamics

The TiDyWAVE is able to generate peak oscillatory velocities between 0.09 and 0.32 m s^{-1}, corresponding to wave periods ranging from 4.0 to 3.5 s, respectively (Fig. 2A). The velocity time series show a sinusoidal-like pattern with slightly higher velocities in the positive direction, like shoaling waves in the nearshore zone. This velocity difference is caused by the pneumatic cylinder which moves slightly faster during the

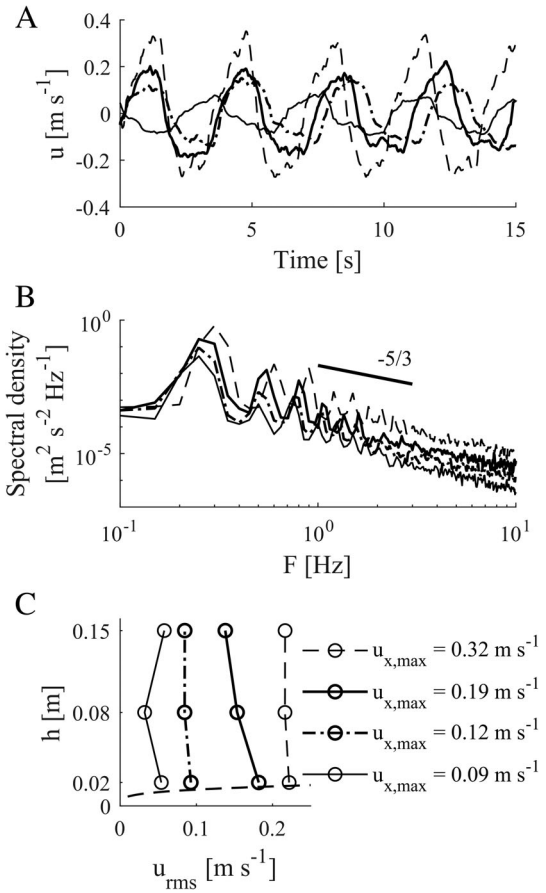

Fig 2. (**A**) Oscillatory velocity time series measured at 0.15 m above the bed for four velocity settings. For clarity only the first 15 s of the time series are plotted, and lines were smoothed by averaging over a 0.1 s moving window. The full, unsmoothed 180-s time series was used for the turbulence spectra and other analyses. (**B**) Corresponding spectral density plots of the flume test runs. (**C**) Root mean square flow velocity profiles. The dashed black line indicates the range where the velocity profile is influence by bottom shear stress according to Eq. 7.

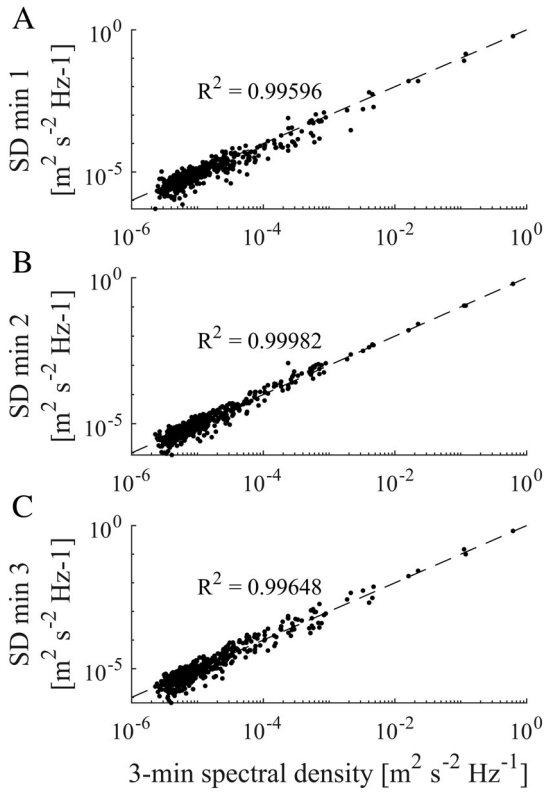

Fig 3. Comparison of the frequency spectrum of the 3-min flow velocity timeseries with $u_{x,max}$ = 0.32 m s^{-1} with the frequency spectra of 1-min windows from the same timeseries: (**A**) minute 1, (**B**) minute 2, and (**C**) minute 3.

"pull" compared to the "push." This is an inherent characteristic of using this type of cylinder for moving water, as the presence of the rod makes the volume smaller on the "pull" side, causing the cylinder to move slightly faster with the same airflow. The vertical U_{rms} profiles (Fig. 2C) show no significant variations over depth. This is in agreement with theory, according to which the bottom boundary layer should be smaller than 0.02 m, the lowest point at which the ADV was placed. Moreover, the rigid paddles force the oscillatory flow to be equal across the vertical.

In all spectral density plots, which show the distribution of wave and turbulent energy over the frequency range (Fig. 2B), there is a clear peak at $F \approx 0.25$ Hz, which corresponds to the wave period of T = 3.5–4 s. The rest of the spectrum follows a slope of −5/3 corresponding to the Kolmogorov inertial subrange, i.e., the dissipation of turbulent energy toward higher frequencies. There are some higher harmonics and reflections visible in the spectrum, but their spectral density is at least 1.12–1.85 (95% confidence interval) orders of magnitude lower than the spectral density of the user-imposed wave. The frequency spectrum did not show any significant changes over time during the measurement period (Fig. 3), indicating an equilibrium between wave and reflection generation and dissipation. This means that the forces on the bed are generated by the user-imposed wave, and that the influence of internal wave reflections and hydrodynamic conditions outside of the flume on turbulence generation is minimal and will stay constant even during longer duration measurements.

Comparing the TiDyWAVE hydrodynamics to natural wave dynamics

Comparing the oscillatory flow in the TiDyWAVE with flow conditions under natural waves (Fig. 4(A,B)) shows that (1) waves in the TiDyWAVE are monochromatic, i.e., very little difference between individual waves in terms of period and velocity, whereas in the field the velocities and periods of individual waves vary, (2) vertical velocity in the TiDyWAVE is small compared to the horizontal velocity and only directed upwards, whereas in the field both vertical and horizontal velocity have nearly the same magnitude, and (3) the peak-oscillatory velocity under the "troughs" of the TiDyWAVE is

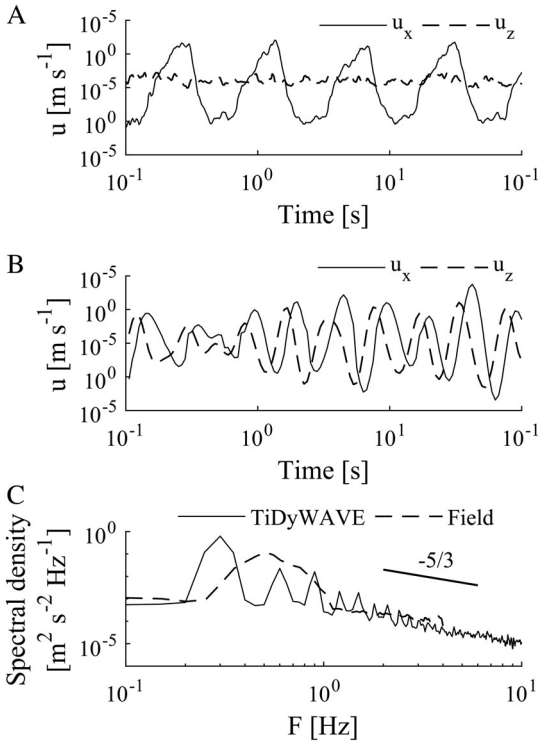

Fig 4. (**A**) Velocity time series measured at 0.15 m above the bed in the TiDyWAVE and (**B**) in the field. For the TiDyWAVE u_{max} is 0.32 m s^{-1}, and for the field measurements the significant peak orbital velocity, defined as the mean of the highest 1/3rd peak orbital velocities, is 0.32 m s^{-1}. (**C**) Corresponding spectral density curves.

maintained for a short period, whereas under natural waves the peak velocity is more instantaneous. (1) translates to a wider energy peak in the frequency spectrum for field waves compared to the oscillatory flow in the TiDyWAVE (Fig. 4C). While (1) is desirable for obtaining accurate measurements, (2) limits the measurement capabilities of the TiDyWAVE to boundary layer process related measurements (e.g., erodibility) only, and (iii) increases A_{max} in the TiDyWAVE compared to natural waves similar in peak orbital velocity and wave period. However, the effect of A_{max} on shear stress generation remains minor and decreases toward higher oscillatory velocities as it only indirectly influences shear stress through the friction factor (see Eq. 8 and 12).

While wave reflection is small in the TiDyWAVE in terms of energy, they are completely absent for field waves (Fig. 4C). The enclosed design for the TiDyWAVE is necessary to prevent leakage, but causes wave reflection and limits the water movement to a fully oscillatory motion. However, both field waves and oscillatory flow in the TiDyWAVE show a clear peak around the peak wave frequency followed by turbulent energy dissipation toward higher frequencies of similar magnitude, indicating that the TiDyWAVE is able to induce the main components of wave energy and is similar to natural waves in terms of turbulent energy magnitude.

Comparing the TiDyWAVE hydrodynamics to the physical design conditions

Figure 5 compares the wave height—period generation capabilities of the TiDyWAVE in its current configuration (u_{max} = 0.32 m s^{-1}) against observed offshore waves in the Western Scheldt and Wadden Sea for three imposed depths (1, 2, and 3 m). With an imposed water depth on 1 m, the TiDyWAVE is able to generate the 19.4% and 15.9% highest waves occurring in the Western Scheldt and Wadden Sea respectively in terms of near-bed peak velocity. However, during the storm surge conditions when the highest waves occur, the water levels on the tidal flats and shoals are generally higher as well, reducing the near-bed peak velocity. Therefore, wave generation percentiles for 1 m water depth are an underestimation. For imposed water depths of 2 and 3 m, the TiDyWAVE is able to generate the near-bed velocities of more extreme waves, the 4.6% and 1.1% highest waves occurring in the Western Scheldt and the 3.8% and 0.7% highest waves occurring in the Wadden Sea. The TiDyWAVE is thus able to generate both the typical near-bed peak velocities during average conditions with low water depth and the extreme near-bed peak velocities during storm conditions corresponding to higher water depths.

Erosion thresholds on bare sediments

On bare sediments, u_{cr} is consistently lower for oscillatory flow compared to unidirectional currents (Fig. 6A). Measured u_{cr} was 47%, 44%, and 33.5% lower under oscillatory flow for the spherical, cylindrical, and moderately sorted sediments, respectively. There is a good correspondence between measured u_{cr} and predicted u_{cr} for spherical sediment specifically, for which the presented theory is strictly valid only, with both the TiDyWAVE, where measured u_{cr} is 1.68 cm s^{-1} higher, and the TiDyFLOW, where measured u_{cr} is 0.79 cm s^{-1} higher. As expected, the cylindrical and moderately sorted sediments generally showed lower predicted u_{cr}-values compared to the measured u_{cr} due to the influences of respectively paving (a grain shape effect) and hiding-exposure mechanisms (a grain sorting effect). For the cylindrical sediment, the measured u_{cr} is 3.04 and 3.50 cm s^{-1} higher than predicted u_{cr} for the TiDyWAVE and the TiDyFLOW, respectively, and for the moderately sorted sediment the measured u_{cr} is respectively 4.47 and 1.8 cm s^{-1} higher. The good correspondence between measured and calculated u_{cr}, specifically for the spherical sediment, implies that the TiDyWAVE can induce near-bed oscillatory motion which is similar to natural near-bed wave motion in both near-bed velocity and turbulence characteristics, which drive the stochastic movement of sediment grains near the erosion threshold and are therefore inherently accounted for in empirical predictors, as they have been derived from flume measurements.

Erosion thresholds on vegetated sediments

Similar to bare sediments, u_{cr} with oscillatory flow is also consistently lower than with unidirectional currents on a *Thalassia testudinum* bed (Fig. 6B). In both cases, u_{cr} increases

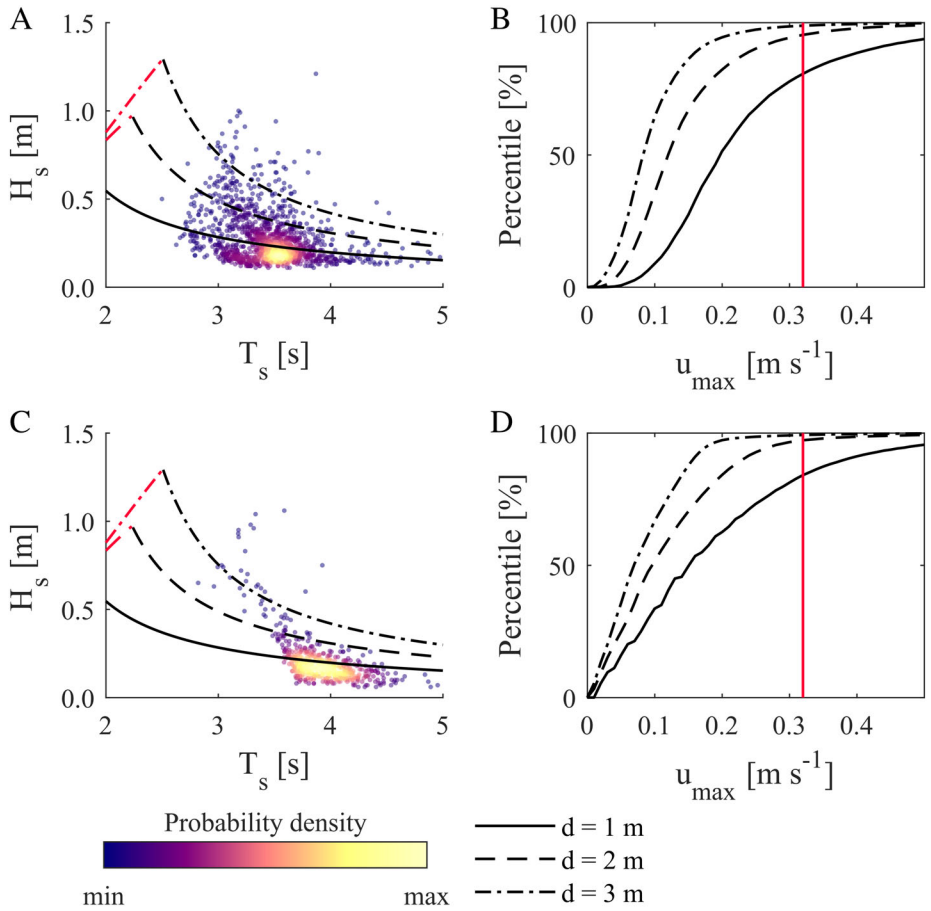

Fig 5. Wave period—Height relations and their relative probability of occurrence for (**A**) the Western Scheldt, and (**C**) the Wadden Sea (dots), and the wave period-height relations of the TiDyWAVE for different imposed depths of 1, 2, and 3 m (lines). The black lines indicate wave height limitation due to the maximum velocity generated by the TiDyWAVE, and the red lines indicate wave height limitation due to wave breaking. u_{max}—Occurrence percentile relations for (**B**) the Western Scheldt, and (**D**) The Wadden Sea at 1, 2 and 3 m depth. For clarity, **A** and **C** show the daily 90th percentile significant wave heights, whereas the full 10-min resolution dataset was used to calculate the percentiles in **B** and **D**.

with increasing blade area (R^2 = 0.86 and R^2 = 0.81 for the TiDyFLOW and the TiDyWAVE, respectively). However, under oscillatory flow u_{cr} increases at a 3.5 times slower rate compared to unidirectional currents. Clearly, the protective effect of seagrass on the sediment is much smaller under wave forcing than when exposed to unidirectional currents. Moreover, u_{cr} under oscillatory flow is lower for the grazed *Thalassia testudinum* compared to bare sediment (Welch's *T*-test p = 0.054), whereas u_{cr} on bare vs. grazed is similar under unidirectional flow (Welch's *T*-test p = 0.364). This indicates that, in short and sparse canopies, seagrasses may have a protective effect under unidirectional flow while erosion is enhanced under oscillatory flow.

Discussion

Opportunities and limitations of oscillatory channels

Current challenges with respect to climate change and nature-based flood defense call for field-based approaches to study ecosystem resilience to hydrodynamic and specifically wave forcing in situ. To be able to determine coastal ecosystem stability under future wave conditions, there is a need for wave-generating field flumes, while so far field flumes have been limited to unidirectional currents only. Here, we have shown that the TiDyWAVE is able to successfully induce near-bed wave motion to measure erosion thresholds of non-breaking waves in situ. The similarity of the turbulence spectra of natural waves and oscillatory flow in the TiDyWAVE and the good correspondence between calculated and measured erosion thresholds of low-density particles, which are particularly sensitive to vertical flow fluctuations induced by pressure gradients, shows that the TiDyWAVE can reproduce the near-bed hydrodynamic processes well enough for measuring erosion thresholds in an ecological setting. Comparing measurements with the TiDyWAVE and a unidirectional field flume (the TiDyFLOW) on *Thalassia testudinum* revealed a large difference in the sheltering capacity of flexible vegetation under wave or current dominated conditions, indicating the

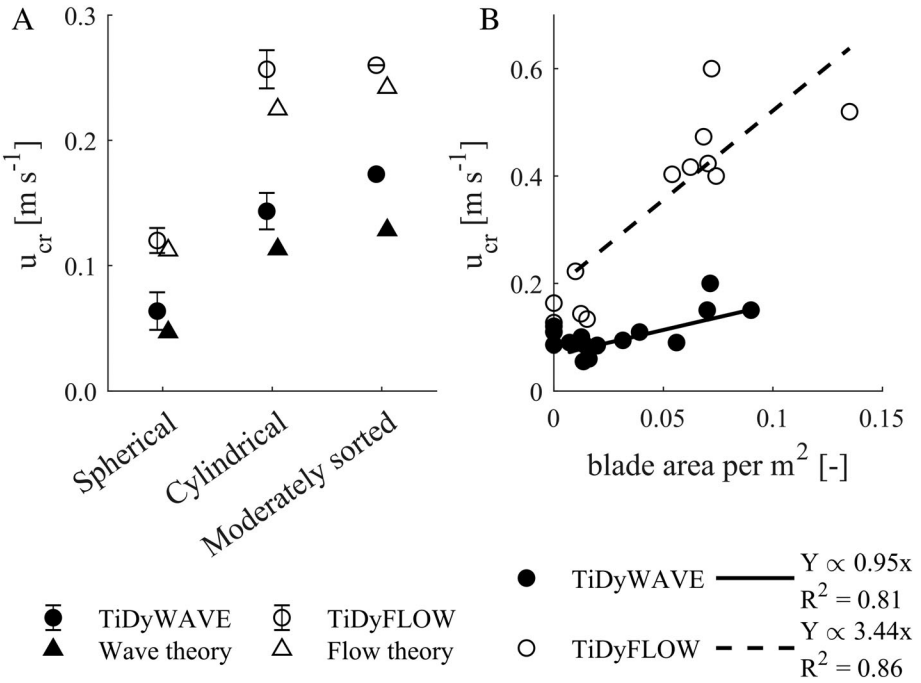

Fig 6. (**A**) Measured and calculated erosion thresholds of the TiDyWAVE and the TiDyFLOW for spherical, cylindrical, and mixed sediments. (**B**) *Thalassia testudinum* blade area per m^2, calculated as shoot density × shoot length × blade width, against u_{cr} measured in the field with the TiDyFLOW and with the TiDyWAVE.

importance of imposing representative hydrodynamic conditions in ecosystem stability studies.

Comparing the TiDyWAVE hydrodynamics to natural conditions

The TiDyWAVE has proven to be easily deployable at various field settings, due to its compact dimensions. Despite giving valuable results, the compact design also imposes some hydrodynamic limitations, which need to be considered. A major difference between oscillatory flow in the TiDyWAVE and orbital flow under natural waves is the absence of vertical velocity in the TiDyWAVE, whereas outside the boundary layer the horizontal and vertical velocity under natural nearshore waves are similar in magnitude (see Fig. 4). This means that oscillatory channels like the TiDyWAVE are not suitable for studying processes affected by flow above the boundary layer (Clubb 2001), such as flocculation and settling of fine sediments or nutrient and gas exchange in the canopy–water interface. Under nonbreaking waves however, the onset of erosion is dominated mainly by turbulence within the boundary layer (Kleinhans and van Rijn 2002; Tinoco and Coco 2018), where vertical flows are near zero. Since the height of the boundary layer remains very small compared to the water depth under short-period waves, oscillatory flow channels can represent near-bed hydrodynamics fairly well (Jonsson and Carlsen 1976).

Estimating u_{cr} within flexible vegetation, using unidirectional vs. oscillatory flow

Comparison with a more traditional unidirectional field flume revealed that a difference in the sheltering mechanisms by flexible vegetation leads to a significant difference in measured u_{cr} on bare sediments and *Thalassia testudinum* beds, which increases with increasing blade area. The "flapping" motion of flexible vegetation under waves allows flows to penetrate through the canopy more easily, increasing shear stress at the bed compared to unidirectional currents with similar energy where the flexible vegetation is deflected downwards, generating a skimming flow over the canopy, shielding the seabed (Koch and Gust 1999; Järvelä 2005). In this study, short canopy *Thalassia testudinum* beds were found to decrease u_{cr} compared to bare sediment under oscillatory flow, whereas no effect was observed under unidirectional flow. Contrastingly, Christianen et al. (2013) reported lower erosion rates, implying higher erosion thresholds, in short canopy *Halodule uninervis* beds compared to bare sediment. However, shoot density was 4–7 times higher (~3350 vs. 480–800 shoots m^{-2}) than this study, indicating in accordance with laboratory flume experiments that a shoot density threshold may determine to which extent short canopy seagrasses reduce or increase erosion (Nepf 2012; Tinoco and Coco 2018), and that this threshold differs between unidirectional and oscillatory flow. Note that in the flume study of Tinoco and Coco (2018)

the near-bed velocity inside the canopy was measured, whereas in this study the velocity above the canopy is measured because (1) it is impossible to reliably obtain detailed boundary layer measurements in the field and (2) the corresponding wave conditions can be calculated directly from the free-stream velocity. Therefore, Tinoco and Coco (2018) observe a decrease of near-bed u_{cr} with increasing shoot density due to increased near-bed turbulence, while in this study an increase of u_{cr} is observed toward higher shoot densities. However, as the measured u_{cr} above the canopy is based on incipient sediment motion inside the canopy, the effect of shoot density on near-bed u_{cr} and the effect of canopy density on flow attenuation are inherently accounted for.

Promising research directions using a field-flume like TiDyWAVE

As is shown in this study, it is possible to measure hydrodynamic thresholds in subtidal marine ecosystems in situ using the TiDyWAVE. The clear Plexiglas walls allow for observation by divers and underwater cameras, and the modular flume design allows for easy fitting of sensors such as ADV's and turbidity loggers. Because of the enclosed design of the flume channel, it is possible to filter the water, allowing for observations of sediment resuspension even in turbid environments. An important application of the TiDyWAVE is the in-situ measurement of erosion thresholds of natural sediments with or without biological structures in wave-dominated environments. Besides measuring erosion thresholds, it is also possible to measure other hydrodynamic thresholds in situ, such as uprooting of aquatic vegetation (Fonseca et al. 1982; Infantes et al. 2011), dislodgement of bivalves (Kangeri et al. 2016), or removal of protective biofilms (Droppo et al. 2007).

Careful consideration however is needed for choosing the ideal flume type for each experiment. Small laboratory flumes such as annular flumes (Widdows et al. 1998; Cozzoli et al. 2018) and wave mesocosms (La Nafie et al. 2012) can be used to conduct high numbers of long-term repeated experiments on the effects of hydrodynamic conditions on specific species. Larger flumes can be used to study hydrodynamic processes in more detail than is possible with the TiDyWAVE, for example detailed boundary layer processes (Butman et al. 1994; Van Duren et al. 2006) and wave attenuation under storm conditions (Möller et al. 2014). However, the ability of the TiDyWAVE to impose specific wave conditions in situ on naturally formed ecosystems makes it a valuable tool to explore (1) the hydrodynamic effects of climate change on coastal ecosystems and (2) to what degree coastal ecosystems remain stable enough for coastal protection purposes.

Technical considerations involved in increasing flume dimensions to generate stronger waves

The configuration of the TiDyWAVE as presented in this study mainly focuses on portability in order to conduct a high number of short-running experiments along ecological gradients in the shallow waters of fetch- or depth-limited coastal systems. However, the TiDyWAVE has been designed with a relatively simple and modular construction, so that it can be scaled. For example, the channel width or height could be increased to accommodate larger structures. Besides shallow subtidal environments, a TiDyWAVE flume could also be applied in deeper waters. The pneumatic components operate best at an air pressure of 10 bar, and can withstand pressures of up to 16 bar, which corresponds to a technical water depth limit of up to 100–160 m. The delay in pressure build up however becomes significant with increasing pneumatic tube length (Sinclair and Robins 1952), which may complicate the control on the movement of the pneumatic cylinder.

For cases where high oscillatory velocities or longer wave periods are needed to induce extreme conditions in more exposed areas than estuaries and shallow basins, the flume length may be increased. Increasing the paddle stroke length will increase the maximum oscillatory velocities and wave periods that the TiDyWAVE can generate. Considering that the piston provides more than enough force, u_{max} is limited by paddle stroke length

$$u_{max} = \frac{1.2\pi l_s}{T} \tag{22}$$

where l_s is the paddle stroke length (m). The factor 1.2 is derived from the difference between u_{max} assuming a fully sinusoidal movement and measured u_{max} for the current configuration of the TiDyWAVE. For example, with a stroke length of 0.9 m u_{max} would be 0.76 and 0.97 m s^{-1} for the Western Scheldt and Wadden Sea, respectively, taking in account that the highest waves have periods in the order of 4.5 and 3.5 s. Vice versa, the maximum wave period could for example also be increased to 6.8 s for a u_{max} of 0.5 m s^{-1}. The portability will however be greatly reduced, as both the length of the bottom plate extension and the measurement area need to be increased accordingly. We suggest a measurement area of at least the length of the orbital magnitude (i.e., the paddle stroke length). Secondly, the presence and scale of bed forms and slope gradients make it increasingly difficult to deploy longer field flumes without compromising the seal with the seabed, which will cause scouring especially during longer-running experiments. Therefore, there are no ideal dimensions for the TiDyWAVE. Rather, it is a trade-off which depends on the specific application and study location that the user has in mind.

Conclusions

The TiDyWAVE is a small, portable field flume capable of inducing near-bed wave motion that was designed based on the proven principle of oscillatory flow channels. It can impose controlled hydrodynamics in situ, which allows for direct measurements of biogeomorphological thresholds in

naturally formed ecosystems. Field flumes are less hydrodynamically accurate than laboratory flumes. However, in situ control of less accurate hydrodynamics is still desirable as hydrodynamics can be quantified, whereas the effect of ecosystem transplantation or formation in laboratory flumes cannot.

This study shows that the TiDyWAVE can generate near-bed flow, shear stress, and turbulence patterns, which are sufficiently similar to natural wave dynamics for ecological studies. This is confirmed by the similarity between natural and flume-generated turbulence spectra and good agreement between measured and predicted u_{cr} for low-density bare sediments, which are particularly sensitive to pressure gradients.

Comparisons between the TiDyFLOW and the TiDyWAVE show the importance of imposing representative water motion, i.e., unidirectional currents or waves, on the ecosystem. The difference in u_{cr} can be explained by theory for bare sediments. However, on marine ecosystems with aboveground structures the theory does not hold. For example, on ecosystems with flexible vegetation the u_{cr}-difference increases with increasing vegetation density, as flexible vegetation is much more efficient in reducing shear stress under unidirectional compared to oscillatory flow.

Data availability statement

The data used in this study is publicly available at 10.4121/uuid:b106b898-2fe6-4a3a-8292-2222fc82dc65.

References

Amos, C. L., J. Grant, G. R. Daborn, and K. Black. 1992. Sea carousel-a benthic, annular flume. Estuar. Coast. Shelf Sci. **34**: 557–577. doi:10.1016/S0272-7714(05)80062-9

Bagnold, R. A. 1946. Motion of waves in shallow water; interaction between waves and sand bottoms. Proc. R. Soc. London. Ser. A Math. Phys. Sci. **187**: 1–18. doi:10.1098/rspa.1946.0062

Bouma, T. J., J. van Belzen, and T. Balke. others 2014. Identifying knowledge gaps hampering application of intertidal habitats in coastal protection: Opportunities & steps to take. Coast. Eng. **87**: 147–157. doi:10.1016/j.coastaleng.2013.11.014

Bouma, T. J., J. van Belzen, and T. Balke. others 2016. Short-term mudflat dynamics drive long-term cyclic salt marsh dynamics. Limnol. Oceanogr. **61**: 2261–2275. doi:10.1002/lno.10374

Bouma, T. J., M. B. De Vries, and P. M. J. Herman. 2010. Comparing ecosystem engineering efficiency of two plant species with contrasting growth strategies. Ecology **91**: 100319061621033. doi:10.1890/09-0690

Butman, C. A., M. Frechette, W. R. Geyer, and V. R. Starczak. 1994. Flume experiments on food supply to the blue mussel *Mytilus edulis*. Limnol. Oceanogr. **39**: 1755–1768. doi:10.4319/lo.1994.39.7.1755

Callaghan, D. P., T. J. Bouma, P. Klaassen, D. van der Wal, M. J. F. Stive, and P. M. J. Herman. 2010. Hydrodynamic forcing on salt-marsh development: Distinguishing the relative importance of waves and tidal flows. Estuar. Coast. Shelf Sci. **89**: 73–88. doi:10.1016/j.ecss.2010.05.013

Camenen, B., A. Bayram, and M. Larson. 2006. Equivalent roughness height for plane bed under steady flow. J. Hydraul. Eng. **132**: 1146–1158. doi:10.1061/(ASCE)0733-9429(2006)132:11(1146)

Camenen, B., M. Larson, and A. Bayram. 2009. Equivalent roughness height for plane bed under oscillatory flow. Estuar. Coast. Shelf Sci. **81**: 409–422. doi:10.1016/j.ecss.2008.11.019

Christianen, M. J. A., J. van Belzen, P. M. J. Herman, M. M. van Katwijk, L. P. M. Lamers, P. J. M. van Leent, and T. J. Bouma. 2013. Low-canopy seagrass beds still provide important coastal protection services. PLoS One **8**: e62413. doi:10.1371/journal.pone.0062413

Clubb, G. S. 2001. Experimental study of vortex ripples in full scale sinusoidal and asymmetric flows. PhD Thesis, Univ. of Aberdeen.

Cozzoli, F., T. J. Bouma, P. Ottolander, M. S. Lluch, T. Ysebaert, and P. M. J. Herman. 2018. The combined influence of body size and density on cohesive sediment resuspension by bioturbators. Sci. Rep. **8**: 1–12. doi:10.1038/s41598-018-22190-3

Droppo, I. G., N. Ross, M. Skafel, and S. N. Liss. 2007. Biostabilization of cohesive sediment beds in a freshwater wave-dominated environment. Limnol. Oceanogr. **52**: 577–589.

Van Duren, L. A., P. M. J. Herman, A. J. J. Sandee, and C. H. R. Heip. 2006. Effects of mussel filtering activity on boundary layer structure. J. Sea Res. **55**: 3–14. doi:10.1016/j.seares.2005.08.001

Fonseca, M. S., J. S. Fisher, J. C. Zieman, and G. W. Thayer. 1982. Influence of the seagrass, *Zostera marina* L., on current flow. Estuar. Coast. Shelf Sci. **15**: 351–364. doi:10.1016/0272-7714(82)90046-4

Ghisalberti, M., and H. M. Nepf. 2002. Mixing layers and coherent structures in vegetated aquatic flows. J. Geophys. Res. **107**: C2. doi:10.1029/2001JC000871

Guza, R. T., and E. B. Thornton. 1980. Local and shoaled comparisons of sea surface elevations, pressures, and velocities. J. Geophys. Res. **85**: 1524–1530. doi:10.1029/jc085ic03p01524

van der Heide, T., E. H. van Nes, G. W. Geerling, A. J. P. Smolders, T. J. Bouma, and M. M. Van Katwijk. 2007. Positive feedbacks in seagrass ecosystems: Implications for success in conservation and restoration. Ecosystems **10**: 1311–1322. doi:10.1007/s10021-007-9099-7

Infantes, E., A. Orfila, T. J. Bouma, G. Simarro, and J. Terrados. 2011. *Posidonia oceanica* and *Cymodocea nodosa* seedling tolerance to wave exposure. Limnol. Oceanogr. **56**: 2223–2232. doi:10.4319/lo.2011.56.6.2223

James, R. K., R. Silva, and B. I. van Tussenbroek. others 2019. Maintaining tropical beaches with seagrass and algae: A promising alternative to engineering solutions. Bioscience **69**: 136–142. doi:10.1093/biosci/biy154

Järvelä, J. 2005. Effect of submerged flexible vegetation on flow structure and resistance. J. Hydrol. **307**: 233–241. doi:10.1016/j.jhydrol.2004.10.013

Jonsson, I. G., and N. A. Carlsen. 1976. Experimental and theoretical investigations in an oscillatory turbulent boundary layer. J. Hydraul. Res. **14**: 45–60. doi:10.1080/00221687609499687

Kangeri, A. K., J. M. Jansen, D. J. Joppe, and N. M. J. A. Dankers. 2016. In situ investigation of the effects of current velocity on sedimentary mussel bed stability. J. Exp. Mar. Bio. Ecol. **485**: 65–72. doi:10.1016/j.jembe.2016.08.011

Kleinhans, M. G., and L. C. van Rijn. 2002. Stochastic prediction of sediment transport in sand-gravel bed Rivers. J. Hydraul. Eng. **128**: 412–425. doi:10.1061/(ASCE)0733-9429(2002)128:4(412)

Koch, E., and G. Gust. 1999. Water flow in tide- and wave-dominated beds of the seagrass *Thalassia testudinum*. Mar. Ecol. Prog. Ser. **184**: 63–72. doi:10.3354/meps184063

Luhar, M., E. Infantes, and H. Nepf. 2017. Seagrass blade motion under waves and its impact on wave decay. J. Geophys. Res. Ocean. **122**: 3736–3752. doi:10.1002/2017JC012731

Marin-Diaz, B., T. J. Bouma, and E. Infantes. 2019. Role of eelgrass on bed-load transport and sediment resuspension under oscillatory flow. Limnol. Oceanogr. lno.11312 **65**: 426–436. doi:10.1002/lno.11312

McGranahan, G., D. Balk, and B. Anderson. 2007. The rising tide: Assessing the risks of climate change and human settlements in low elevation coastal zones. Environ. Urban. **19**: 17–37. doi:10.1177/0956247807076960

Miche, M. 1944. Mouvements ondulatoires de la mer en profondeur constante ou décroissante, p. 369–406. *In* Annales de ponts et chaussees. École nationale des ponts et chaussées. 6fceef55-d71b-4e3e-a94f-98ff17cb8f91.

Möller, I., M. Kudella, and F. Rupprecht. others 2014. Wave attenuation over coastal salt marshes under storm surge conditions. Nat. Geosci. **7**: 727–731. doi:10.1038/ngeo2251

Morim, J., M. Hemer, and X. L. Wang. others 2019. Robustness and uncertainties in global multivariate wind-wave climate projections. Nat. Clim. Chang. **9**: 711–718. doi:10.1038/s41558-019-0542-5

La Nafie, Y. A., C. B. de los Santos, F. G. Brun, M. M. van Katwijk, and T. J. Bouma. 2012. Waves and high nutrient loads jointly decrease survival and separately affect morphological and biomechanical properties in the seagrass *Zostera noltii*. Limnol. Oceanogr. **57**: 1664–1672. doi:10.4319/lo.2012.57.6.1664

Nepf, H. M. 2012. Hydrodynamics of vegetated channels. J. Hydraul. Res. **50**: 262–279. doi:10.1080/00221686.2012.696559

Nyberg, B., and J. A. Howell. 2016. Global distribution of modern shallow marine shorelines. Implications for exploration and reservoir analogue studies. Mar. Pet. Geol. **71**: 83–104. doi:10.1016/j.marpetgeo.2015.11.025

O'Donoghue, T., and G. S. Clubb. 2001. Sand ripples generated by regular oscillatory flow. Coast. Eng. **44**: 101–115. doi:10.1016/S0378-3839(01)00025-4

Peralta, G., L. van Duren, E. Morris, and T. Bouma. 2008. Consequences of shoot density and stiffness for ecosystem engineering by benthic macrophytes in flow dominated areas: A hydrodynamic flume study. Mar. Ecol. Prog. Ser. **368**: 103–115. doi:10.3354/meps07574

Ribberink, J. S., J. J. van der Werf, T. O'Donoghue, and W. N. M. Hassan. 2008. Sand motion induced by oscillatory flows: Sheet flow and vortex ripples. J. Turbul. **9**: 1–32. doi:10.1080/14685240802220009

Van Rijn, L. C. 1993. Principles of sediment transport in rivers, estuaries and coastal seas. Aqua publications.

Rupprecht, F., I. Möller, and M. Paul. others 2017. Vegetation-wave interactions in salt marshes under storm surge conditions. Ecol. Eng. **100**: 301–315. doi:10.1016/j.ecoleng.2016.12.030

Scoffin, T. P. 1968. An underwater flume. J. Sediment. Petrol. **38**: 244–246.

Sinclair, A. R., and A. W. Robins. 1952. A method for the determination of the time lag in pressure measuring systems incorporating capillaries. Natl. Advis. Comm. Aeronaut. Tech. Note 2793.

Soulsby, R. 1997. Dynamics of Marine Sands: A manual for practical applications. Thomas Telford Ltd.

Swart, D. H. 1976. Predictive Equations Regarding Coastal Transports. *15th International Conference on Coastal Engineering*. American Society of Civil Engineers. 1113–1132.

Temmerman, S., P. Meire, T. J. Bouma, P. M. J. Herman, T. Ysebaert, and H. J. De Vriend. 2013. Ecosystem-based coastal defence in the face of global change. Nature **504**: 79–83. doi:10.1038/nature12859

Tinoco, R. O., and G. Coco. 2018. Turbulence as the main driver of resuspension in oscillatory flow through vegetation. Case Rep. Med. **123**: 891–904. doi:10.1002/2017JF004504

Tolhurst, T. J., R. Riethmüller, and D. M. Paterson. 2000. In situ versus laboratory analysis of sediment stability from intertidal mudflats. Cont. Shelf Res. **20**: 1317–1334. doi:10.1016/S0278-4343(00)00025-X

Widdows, J., M. D. Brinsley, N. Bowley, and C. Barrett. 1998. A benthic annular flume for in situ measurement of suspension feeding/biodeposition rates and erosion potential of intertidal cohesive sediments. Estuar. Coast. Shelf Sci. **46**: 27–38. doi:10.1006/ecss.1997.0259

Widdows, J., P. L. Friend, A. J. Bale, M. D. Brinsley, N. D. Pope, and C. E. L. Thompson. 2007. Inter-comparison between five devices for determining erodability of intertidal

sediments. Cont. Shelf Res. **27**: 1174–1189. doi:10.1016/j.csr.2005.10.006

Acknowledgments

The TiDyWAVE was originally designed by Tjeerd Bouma and Bert Sinke, built by the technical workshop of the NIOZ and tested and optimized in hydrodynamics and pneumatic control by Jaco de Smit. We thank Daniel Blok, Jeroen van Dalen, Lennart van IJzerloo, and Jan Megens for their practical assistance in conducting the lab experiments. The in-situ erosion threshold dataset is part of a larger field campaign conducted with Liesbeth Bakker, Marjolijn Christianen, Rebecca James, and Marieke van Katwijk under permit from Openbaar Lichaam Bonaire nr. 558/2015-2015007762. Eduardo Infantes kindly provided the field ADV data and the photograph of the TiDyWAVE during in-situ deployment. Three anonymous reviewers provided constructive feedback improving the manuscript. For more information on building the TiDyWAVE, please contact tjeerd.bouma@-nioz.nl.

Submitted 01 April 2020
Revised 01 July 2020
Accepted 11 July 2020

Associate editor: Xiao Hua Wang